



Interaction Between the Notch and Mortar–Mortar Interface (with Different Inclinations) in Semi-Circular Bend Specimens

Jinwei Fu¹ · Hadi Haeri² · Vahab Sarfarazi³ · Mohammad Fatehi Marji⁴

Received: 1 September 2021 / Accepted: 17 October 2021 / Published online: 3 November 2021
© Shiraz University 2021

Abstract

The effects of interaction between edge crack (notch) with the mortar–mortar interface on the mechanical behaviour of the semi-circular bend (SCB) specimens were considered in this study. The SCB specimens with different angles of mortar–mortar interface and different joints' lengths were measured experimentally. These SCB specimens with 10 cm in diameter and with edge cracks of different lengths were prepared and tested in the laboratory under the applied force rate of 0.004 mm/min. The tensile strength of interface was 0.15 MPa and the joints' tensile fracture toughness was 0.28 MPa√m. These tests showed that the joint (notch) lengths and the interface angles (related to the loading direction) mostly govern the process of failure and fracturing of the SCB specimens. Also, the particle flow code in PFC2D was used to simulate the experimentally tested SCB specimens. Furthermore, one vertical joint (edge crack) with different lengths (i.e. 0.5, 1, 2, 3, 3.5 and 4 cm) was created in each model. It has been shown that the specimens' fracture toughness is highly affected by the length of the edge crack and the direction (angle) of mortar–mortar interface. Also, the tensile strength of the model is related to the number of induced tensile cracks in the joint and the interface. The tensile cracks increase with decrease in the joint length and increase in the interface angle. The model breakage occurs along with the interface and there is no failure at the tip of the crack for the interface angle of less than 60°. On the other hand, the fracture toughness of samples is constant by increasing the joint length for the interface angles of 60°, 75° and 90°.

Keywords Mortar–Mortar interface · Joint length · Interface angle · PFC2D · Semi-circular bend (SCB) test

1 Introduction

The mechanical behaviour of most concretes and rocks are usually concerned with the determination of their fracture toughness as measured in the laboratory or approximated numerically. For these brittle materials, the fracture toughness of Mode-I is usually measured through various

experimental tests in the laboratory. Recently, some methods of testing are developed by many investigators to calculate the fracture toughness (Keles and Tutluoglu 2011; Tutluoglu and Keles 2011; Adiyaman 2015; Haeri et al. 2017; Fang and Fall 2020; Golewski 2021a, b, c). Most of these methods use the core samples and can be classified as the cylindrical, disc and semi-disc configurations as far as the specimens' shape is concerned. In 1988, Ouchterlony proposed the Chevron Bending (CB) and Short Rod (SD) methods for measuring the rocks' fracture toughness. Both of these methods require relatively intact and long cores for measuring the fracture toughness of rocks (Cui et al. 2010). However, the other disadvantages of these methods may include the complexity of the setup test and the need for expensive testing apparatus (Fowell and Chen 1990; Dai et al. 2011, Bi 2016). Some new researchers compared their experimental and numerical studies with the results obtained by the suggested methods, such as the short rod (SR) method. In this method, the direction of the applied tensile load is perpendicular to that of the chevron notch (Li

✉ Vahab Sarfarazi
vahab.sarfarazi@gmail.com

¹ School of Civil Engineering and Transportation, North China University of Water Resources and Electric Power, Zhengzhou 450046, China
² State Key Laboratory for Deep GeoMechanics and Underground Engineering, Beijing 100083, China
³ Department of Mining Engineering, Hamedan University of Technology, Hamedan, Iran
⁴ Department of Mine Exploitation Engineering, Faculty of Mining and Metallurgy, Institute of Engineering, Yazd University, Yazd, Iran

et al. 2015; Zhou et al. 2015; Öner 2015; Yaylac 2016; Sarfarazi 2016; Haeri et al. 2017; Shou 2019a, 2019b). These constraints may minimize the chance of obtaining the same fracture toughness for a material through different tests. On the other hand, these ISRM methods may provide some consistent fracture toughness, but in many cases, there are about 20 to 30% variations in the measured values reported for both CB and SR methods (Iqbal and Mohanty 2007). The second-class focus is on the Brazilian disc (BD) type specimens usually known as Brazilian Disc (BD) method and used by many investigators in the recent decades (Dai et al. 2010, 2011; Kourkoulis et al. 2012; Yaylaci 2013; Ghazvinian et al. 2013; Haeri et al. 2017; Zhou 2014; Zhou et al. 2015; Yaylaci 2016; Shou 2021; Yaylaci 2020; Yaylaci 2021a, b, c). The Brazilian disc type specimens with cracks and holes have also been used for measuring the critical stress intensity factor of Mode I, such as (a) the double-edge-cracked Brazilian disc (DECBD), the cracked straight through Brazilian disc (CSTBD), and the flattened Brazilian disc (FBD) methods (Chen et al. 2008; Keles and Tutluoglu 2011; Markides and Kourkoulis 2020; Chen et al. 2005; Yu et al. 2021); (b) The holed cracked flattened Brazilian disc (HCFBD), The holed-flattened Brazilian disc (HFBD), the hollow centre-cracked disc (HCCD) methods (Yang 2015; Tang et al. 1996), (c) the method suggested by Shiryaev and Kotkis (1982) known as the radial cracked ring-type method and the most frequently used ISRM suggested method as the cracked chevron notched Brazilian disc (CCNBD) specimen (Wang et al. 2012; Wei et al. 2015; Du et al. 2017). Several methods were also proposed for the determination of the Mode I and Mode II fracture toughness (Fowell et al. 2006; Fang and Fall 2020; Vălean et al. 2020; Golewski 2021a).

The third class methods mainly used the semi-disc type specimens with notch, e.g. the cracked chevron notched semi-circular bend (CCNSCB) and the notched semi-circular bend (NSCB) methods (Fowell and Chen 1990; Kuruppu and Chong 2012; Zhou et al. 2012; Kuruppu et al. 2014; Zhou et al. 2012; Wei et al. 2015; Du et al. 2017). The geomaterials' fracture toughness for the mixed loading conditions can be measured by these methods (Kuruppu and Chong 1986). In the third method, the NSCB method is the most popular one as compared to the CCNSCB method. Kuruppu et al. (2014) proposed that the SCB specimens, as shown in Fig. 1, may be added to the suggested methods for measuring rock fracture toughness.

In the third method, the SCB specimens are prepared from the cores and therefore, require a little machining effort. These cores are in compact form and can be cut into slices to provide the suitable semi-circular discs. The SCB specimens are more convenient to study the effects of various physical and mechanical parameters, such as moisture content, temperature, time and strain rate on the geo-materials' fracture toughness. The following relations are usually

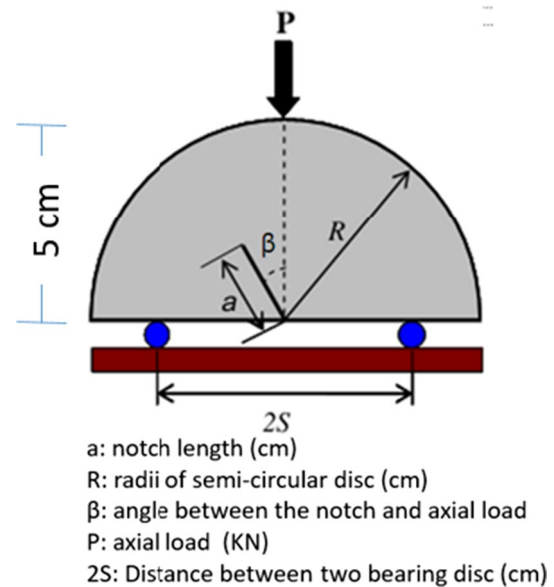


Fig. 1 Geometrical and loading configuration of the Semi-circular bends (SCB) specimens (Kataoka et al. 2014)

suitable for estimating the fracture toughness (K_{IC}) from the SCB specimens (Kuruppu et al. 2014).

$$K_{IC} = \frac{P_{max}\sqrt{\pi a}}{2rt} Y_I \left(\frac{a}{R}, \frac{S}{R} \right) \quad (1)$$

$$Y_I = \frac{S}{R} (2.91 + 54.39\beta - 391.4\beta^2 + 1210.6\beta^3 - 1650\beta^4 + 875.9\beta^5) \quad (2)$$

where P_{max} is the applied load at failure, a is the crack length, r and t represent the radius and thickness of the SCB specimen, respectively. In this equation, the geometrical stress intensity factor, Y_I is written in a non-dimensional form considering the S/R ratio which is the ratio of the support span S to the radius R and the ratio, $\beta = a/R$ is the non-dimensional notch length (Kuruppu et al. 2014). The factor Y_I is calculated by several researchers for either analytical or numerical techniques (e.g. Kuruppu and Chong 1986). In the previous researches, the interaction between the mortar–mortar interface and edge notch in SCB test has not been fully considered. The main aim of this paper is to consider the effects of various parameters, such as interface angles and edge crack lengths on the failure mechanism of mortar SCB specimens. However, experimental and numerical methods are used to assure the accuracy and validity of the results. Although numerical results are tested to be valid through the experimental results, in these analyses, the ability of PFC in simulating the interaction between mortar–mortar interface and edge notch in SCB specimens is also approved. It should be noted that some extra numerical models can be made in PFC for further analyses and there is

no need for doing more experimental tests. These analyses also explain that which one of the notches or the interface may mobilize the failure process of the SCB specimens.

2 Experimental Investigation

The experimental tests were conducted in the laboratory on the specially prepared SCB type mortar specimens under compressive loading.

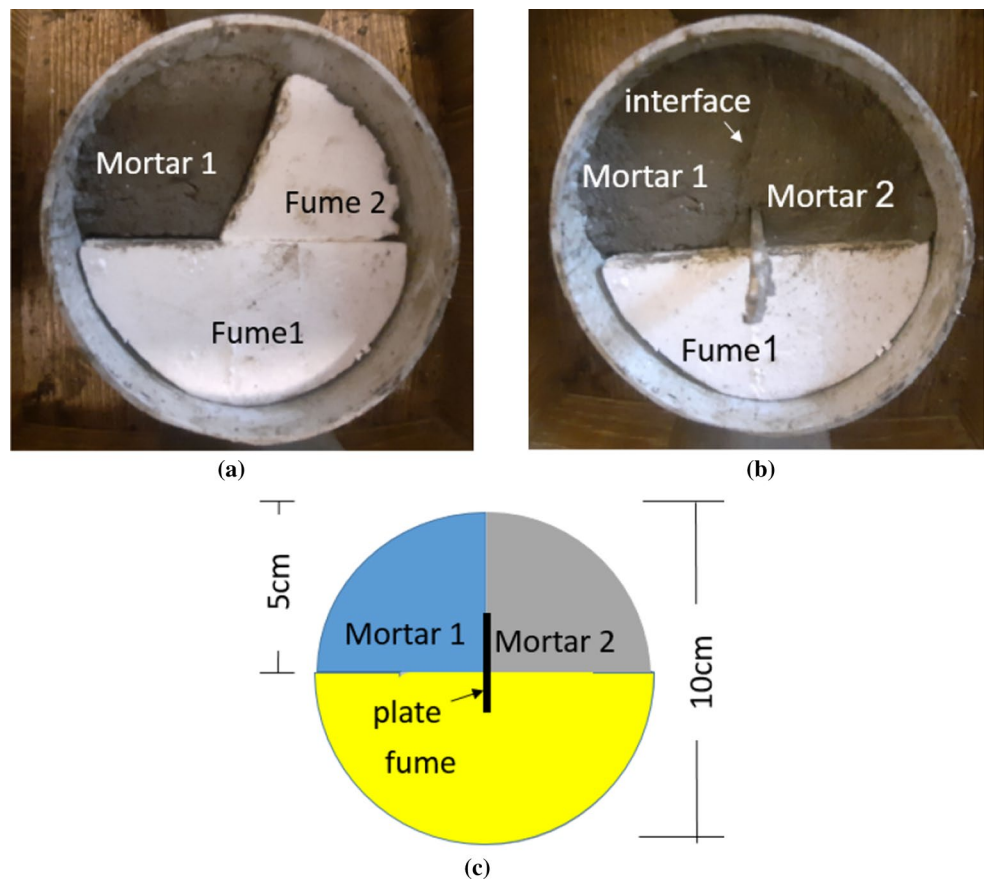
2.1 Preparing the SCB Specimens with Edge Crack

Gypsum, cement, sand and rock debris are the main geo-materials that can be used to prepare rock-like, concrete and mortar specimens for investigating their fracture and failure mechanism under various loading conditions. Some concrete specimens with the pre-existing cracks were tested experimentally by many investigators to analyse the cracks extensions scenarios in quasi-rocks (Shemirani et al. 2016; Golewski and Sadowski 2017; Golewski 2019a; Golewski 2019b; Dastgerdi et al. 2020; Hu et al. 2020; Yaylacı 2020; Wang et al. 2021; Shen et al. 2021; Zhang et al. 2021; Lv et al. 2021; Saha and Sagar 2021). In this study, the SCB specimens of mortar (concrete-like materials) were prepared

in the laboratory by properly mixing the cement (PPC) and fine sand with water. Both the thickness and diameter of the Brazilian discs prepared for the experimental tests were selected to be 100 mm as shown in Fig. 2a–c.

In order to make the SCB specimens, first a plastic cylinder was selected and a longitudinal groove was created in it. This groove helps the physical sample to come out easily from the sealer. Foam No. 1 was placed in the form of a half-cylinder on the bottom of the plastic cylinder as shown in Fig. 2a. This foam divides the cylindrical space into two parts (for making semi-disc type specimens). To create a joint between two mortars with an ideal angle, foam No. 2 was placed inside the cylindrical space with a desired cutting angle (Fig. 2a). To create the edge crack, an aluminium blade with a thickness of 1 mm, a height of 10 cm and an ideal length was placed in foam 1. So that half of the blade was in foam 1 and the other half was in the open space as shown in Fig. 2b. The remaining space was filled with mortar 1. When mortar 1 hardened, foam 2 was removed from the cylinder and replaced with mortar 2 (Fig. 2b). Then, as mortar 2 hardened, first the blade came out of foam 1 and then foam number 1 was removed from the mould. In this way, a specimen containing an interface and an edge crack was created in the mould. It is worth mentioning that the mould was greased so that the casted specimen can be removed easily from it. The length of the blades is 1, 2, 3

Fig. 2 **a** Plastic cylinder containing foam no. 1 and foam no. 2 and mortar 1, **b** mortar–mortar interface, **c** schematic view of fume, plate and mortars



and 4 cm, respectively, which is intended to create the edge cracks of different lengths. Also, by changing the slope angle of foam 2, the interfaces with different inclination angles can be created in the specimens. Figure 2c shows a schematic view of the specimens' preparing procedure.

The Semi-Circular Bend (SCB) specimens with different angles of mortar–mortar interfaces and various joints' lengths are prepared in the form of Brazilian discs.

The mortar–mortar interface angles of 15°, 30°, 45°, 60°, 75° and 90° are generated in the specimens. Also, the edge cracks are produced within the specimens with a thin steel shim of 1 mm thickness which is inserted in the mould during the specimen casing process. During the specimens' casting, it is possible to provide edge cracks of different lengths (i.e. 0.5, 1, 2, 3, 3.5 and 4 cm) in the specimens. The applied force can be uniformly distributed in the top and bottom of the specimen at a rate of 0.004 mm/min.

The specimens containing interfaces with different angles of 15°, 30°, 45°, 60°, 75° and 90°, and with different lengths of edge cracks are shown in Fig. 3a–h, respectively. These interface geometries are characterized by α and L parameters, to express the angles of mortar–mortar interfaces and the lengths of edge cracks, respectively.

2.2 Experimental Results of the SCB Tests on Mortar Specimens

The SCB specimens containing the edge cracks (with different lengths) and also having different mortar–mortar interface angles are properly made in the laboratory and prepared for experimental tests. Totally, three types of cracks were initiated in modelled samples i.e. tensile cracks, shear cracks and the mixed tensile/shear cracks. It was shown that when the angle of mortar–mortar interface was less than 30°, shear cracks were developed through this interface and, when the angle of mortar–mortar interface was 45°, the mixed mode cracks were produced in both of the interface and the intact material. On the other hand, when the angle of mortar–mortar interface was more than 45°, the tensile cracks were developed in the intact material (Fig. 4a–h). It should be noted that when the notch (edge crack) was situated in mortar 2, only one tensile crack initiates from the notch tip and propagates parallel to the loading axis till it meets the sample boundary. Also, after the test, it was observed that the failure surface was smooth (without pulverized material) which indicated a tensile failure process in the material sample.

2.3 Calibrating the SCB Models for the Numerical Simulation

The properties of the mortar–mortar interfaces in the SCB specimens were calibrated for PFC2D software. The

calibrated normal and shear bonds were 4 MPa and the calibrated friction coefficient was 0.5. The contact bonds were used because of the low strength of mortar–mortar interface. The porosity was kept as 0.08 and local damping in the numerical model was equal to 0.7. The failure patterns for the experimental tests and for the numerical modelling of the edge notch interaction with the mortar–mortar interface of 0° angle are shown in Fig. 5a–c. As shown in these figures, the tensile failure may occur at the mortar–mortar interfaces of the SCB specimens in the laboratory tests and also in their numerical modelling counterparts. The values of the experimental and numerical tensile strengths of the interface were 0.15 MPa and 0.12 MPa, respectively. Therefore, it is evident that there is good accordance between the results obtained experimentally and numerically in this research work.

Figure 6a–c shows the failure patterns of the experimental tests and numerical simulations in the SCB specimens considering a crack length of 1 cm. In these figures, the black lines represent the tensile cracks. They also illustrate that the tensile fracture is dominant in the SCB specimens. The fracture toughness of the SCB specimens may be calculated from these experimental and numerical results. Again, these results demonstrate that there are good agreements between the experimentally obtained results with those approximated in the numerical outputs.

The calibrated PFC2D was adopted for the numerical solution of the Semi-Circular Bend Specimens with different angles of mortar–mortar interfaces and different edge crack's lengths (Fig. 7a–h). The approximated numerical results given in Fig. 7a–h allow for different angles of mortar–mortar interfaces and edge crack's lengths. These estimated results (i.e. Fig. 7a–e) were compared with those already given by the experimental tests (i.e. Fig. 4a–e), respectively. Then, tensile fracture toughness in the numerical simulation and tensile fracture toughness in the experimental test were obtained as 0.3 MPa \sqrt{m} and 0.28 MPa \sqrt{m} , respectively. It has been visualized that there is a relatively good agreement between the numerically simulated results with those measured experimentally through laboratory tests.

3 Numerical Tests

3.1 Numerical Modelling of the Mortar–Mortar Interface and internal Joint

The numerical software, PFC2D, is calibrated for adopting the proper micro-parameters and used to simulate the SCB tests for investigating the effects of interaction between mortar–mortar interface and edge crack (open joint) on the breaking mechanism of the mortar (Figs. 8, 9, 10, 11, 12, 13). In these analyses, the PFC specimen had the diameter

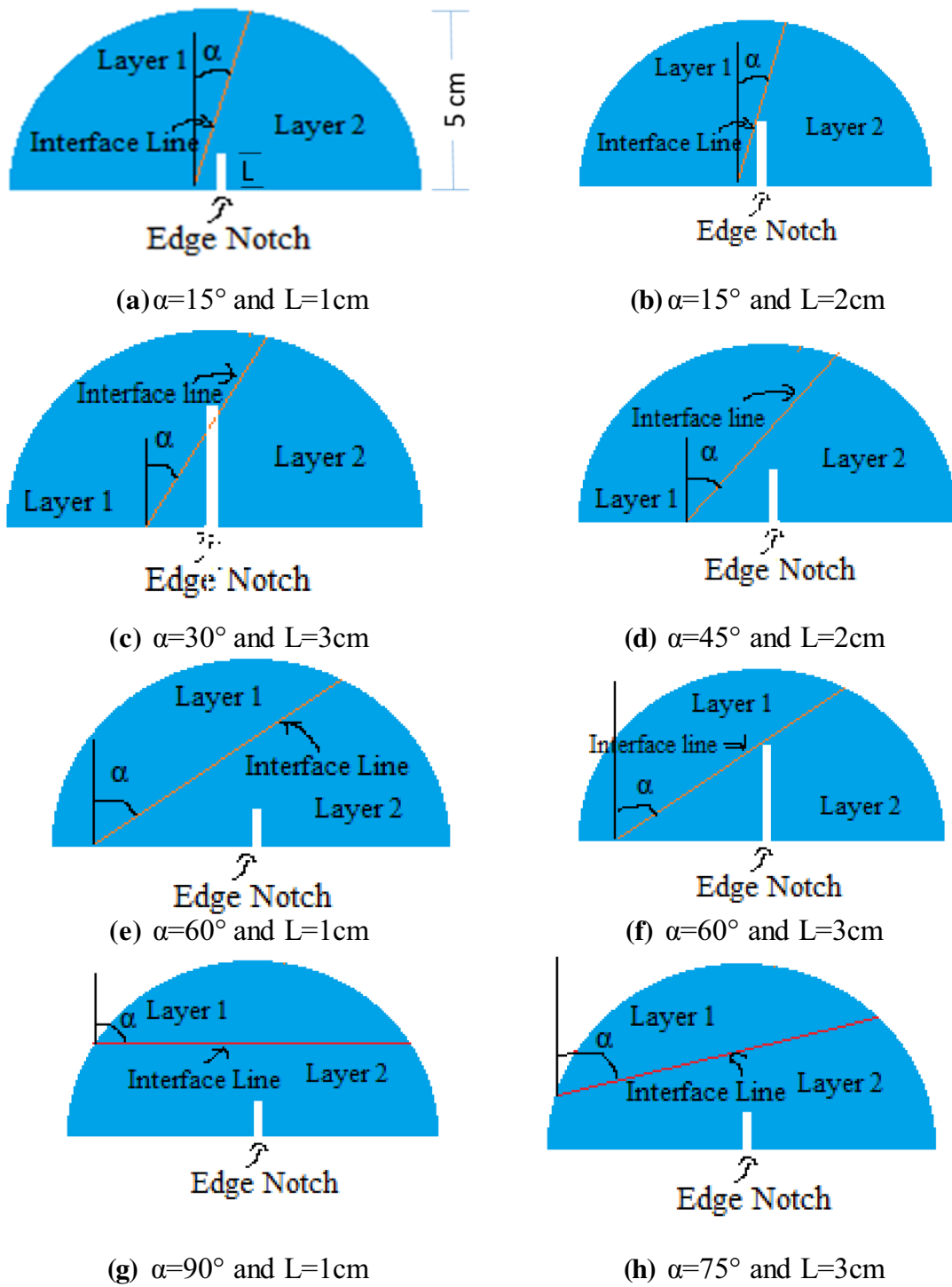


Fig. 3 Geometries show different angles of mortar–mortar interface and the lengths of edge cracks for the SCB specimens

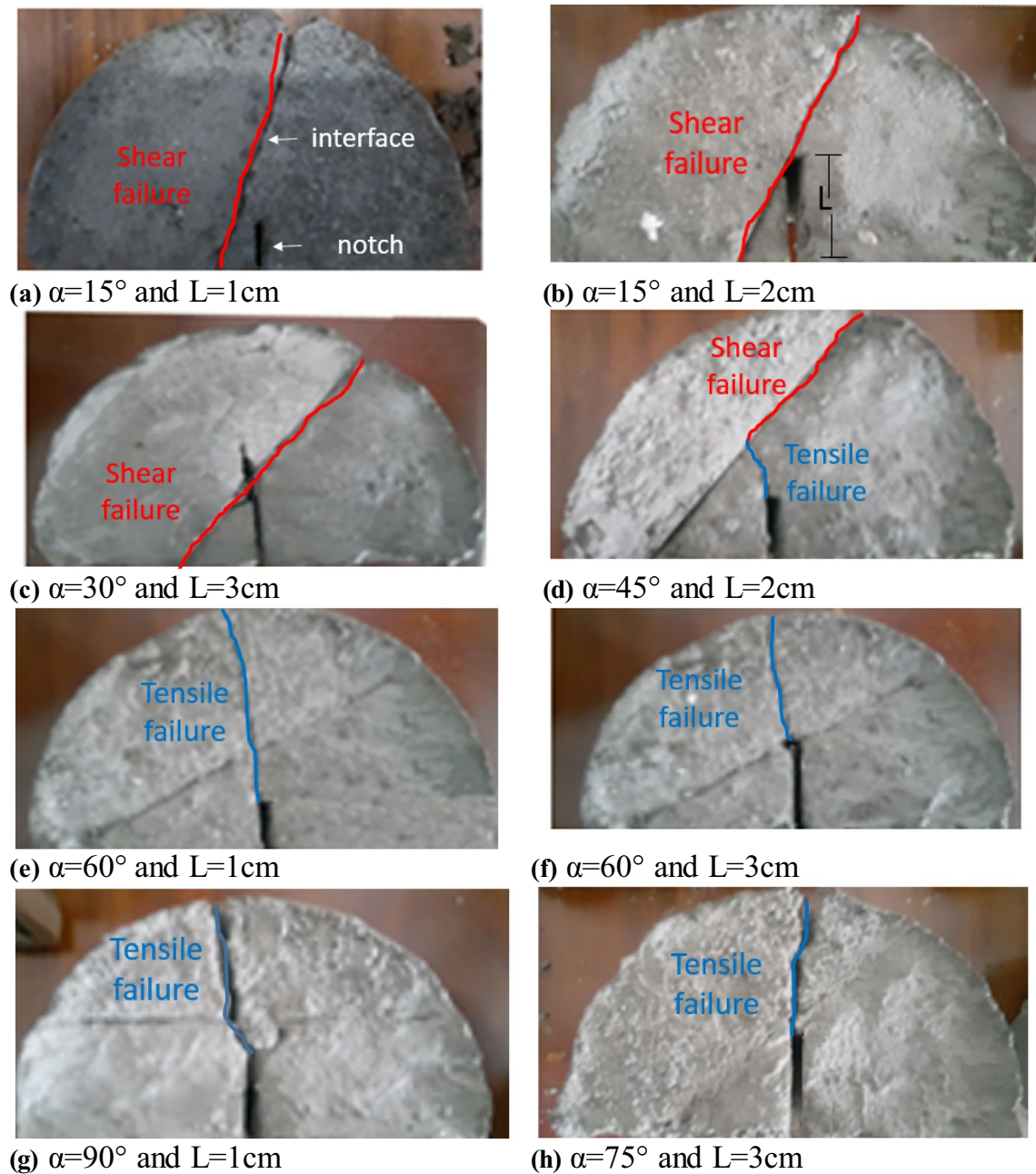


Fig. 4 Failure patterns occurred in the SCB Specimens with different mortar–mortar interface inclinations and various edge crack lengths

of 100 mm. The micro-parameters for mortar were applied into the model. The interfaces with different angles of 15° , 30° , 45° , 60° , 75° and 90° were created in the models. Also, the edge cracks were created by deleting the particle bands at the specified location of the model. The lengths of different edge cracks (joints) varied as: 0.5, 1, 2, 3, 3.5

and 4 cm, and their opening was kept constant as 1 mm. The force was applied at the upper and lower walls of the modelled specimen. This force was registered on the upper wall of the sample by considering the reaction forces on this wall. Totally 36 numerical tests were simulated in this study.

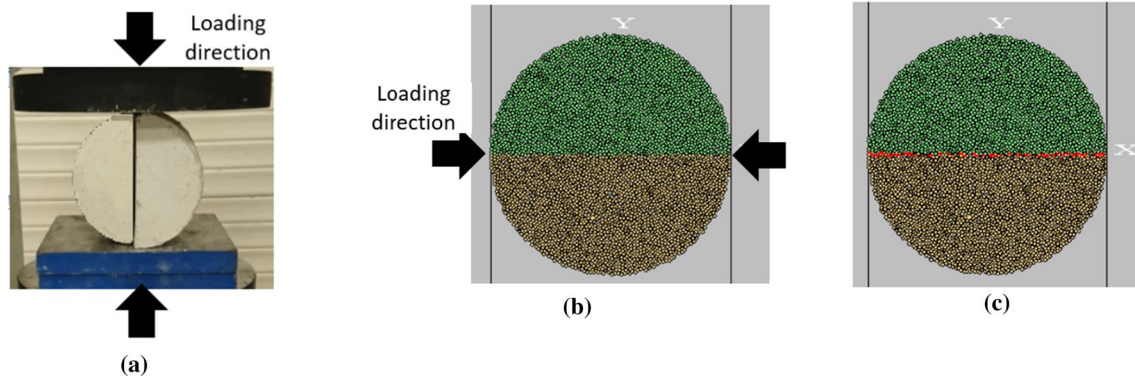


Fig. 5 Experimental and numerical mortar–mortar interfaces **a** experimental tensile failure at the interface, **b** numerically simulated interface, **c** numerically modelled tensile failure at the interface

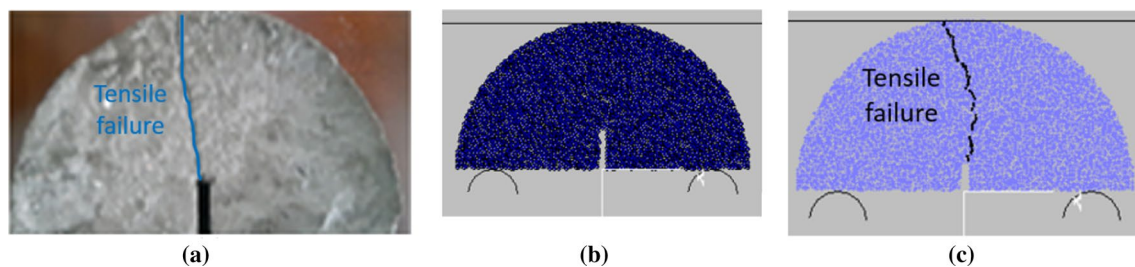


Fig. 6 Tensile failure of mortar specimen **a** as observed in the experimental test, **b** the numerical modelling of the specimen, **c** Tensile failure in modelled specimen

3.2 Effects of Joints' Lengths and Interface Angles on the Specimens' Failure Process

The modelled SCB specimens containing various interface angles and different crack lengths are considered to study the breaking process of the brittle geo-materials.

3.2.1 The Simulated SCB Specimens Considering 15° Mortar–Mortar Interface Angle

Figure 14a–f shows the fracturing pattern of the modelled specimens with the interface angle of 15°. The length of joints was 0.5 cm (Fig. 14a), 1 cm (Fig. 14b), 2 cm (Fig. 14c), 3 cm (Fig. 14d), 3.5 cm (Fig. 14e) and 4 cm (Fig. 14f). The red and black lines demonstrate the wing (tensile) cracks and secondary (shear) cracks, respectively. As shown in Fig. 14, the failure process of the SCB specimens is mainly due to the induced tensile cracks originating from the model interface and propagating along with it. Therefore, it can be deduced that in the SCB mortar specimens, the tensile mode of fracture is more dominant compared to that of the shear mode.

3.2.2 The Modelled Mortar–Mortar Interface with a 30° Interface Angle

Figure 15a–f demonstrates the mechanism of failure in the simulated mortar–mortar samples with 30° interface angle. In this analysis, the joints' lengths were 0.5 cm (Fig. 15a), 1 cm (Fig. 15b), 2 cm (Fig. 15c), 3 cm (Fig. 15d), 3.5 cm (Fig. 15e) and 4 cm (Fig. 15f). In these figures, the red lines show the induced primary cracks and the black lines show the secondary cracks. However, it has been shown that the tensile cracks are the main cause of failure in these modelled specimens.

3.2.3 The Modelled Mortar–Mortar Interfaces in the Specimens with 45° Interface Angle

Figure 16a–f demonstrates the mechanism of failure and the fracture patterns in the mortar–mortar interface of the simulated SCB specimens with 45° interface angle. The lengths of joints were selected as 0.5 cm (Fig. 16a), 1 cm (Fig. 16b), 2 cm (Fig. 16c), 3 cm (Fig. 16d), 3.5 cm (Fig. 16e) and 4 cm (Fig. 16f). In these figures, tensile cracks are denoted by red

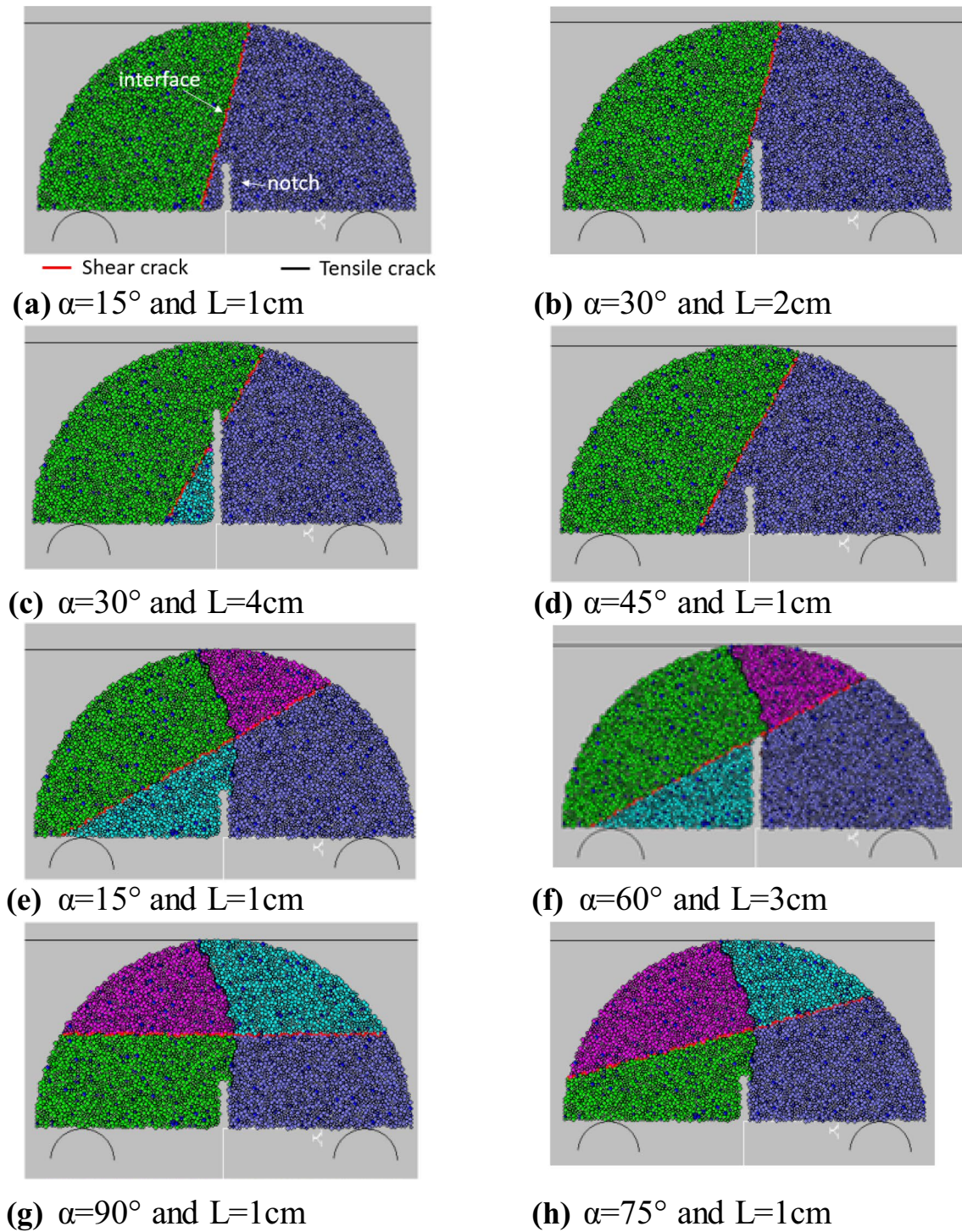


Fig. 7 Numerically (PFC2D) estimated failure process for the SCB specimens with different interface angles (α) and edge crack (joint) lengths (L); **a** $\alpha=15^\circ$ and $L=1\text{ cm}$, **b** $\alpha=30^\circ$ and $L=2\text{ cm}$, **c** $\alpha=30^\circ$

and $L=4\text{ cm}$, **d** $\alpha=45^\circ$ and $L=1\text{ cm}$, **e** $\alpha=15^\circ$ and $L=1\text{ cm}$, **f** $\alpha=60^\circ$ and $L=3\text{ cm}$, **g** $\alpha=90^\circ$ and $L=1\text{ cm}$ and **h** $\alpha=75^\circ$ and $L=1\text{ cm}$

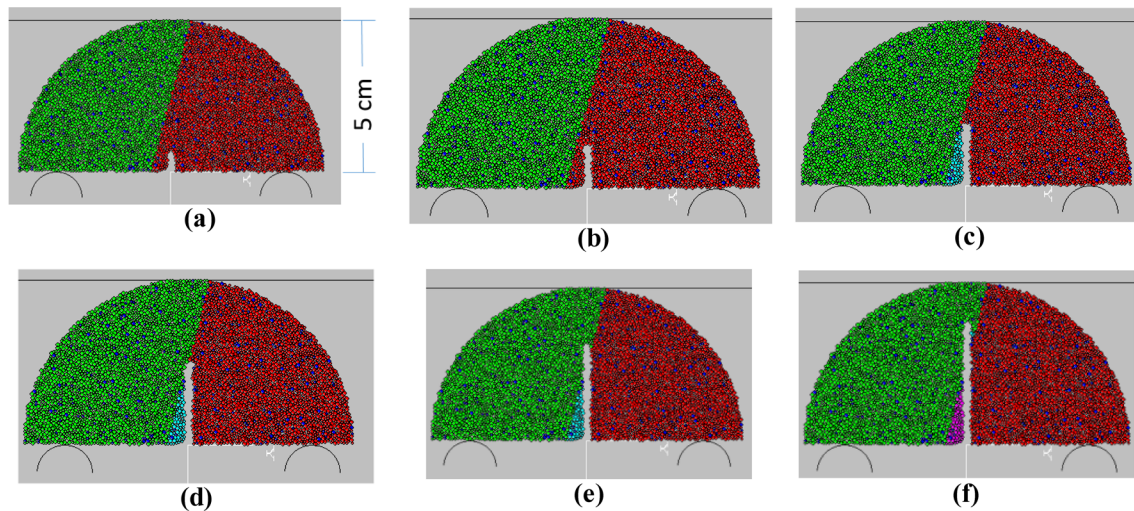


Fig. 8 Model with interface angle of 15° and different joint (edge crack) lengths

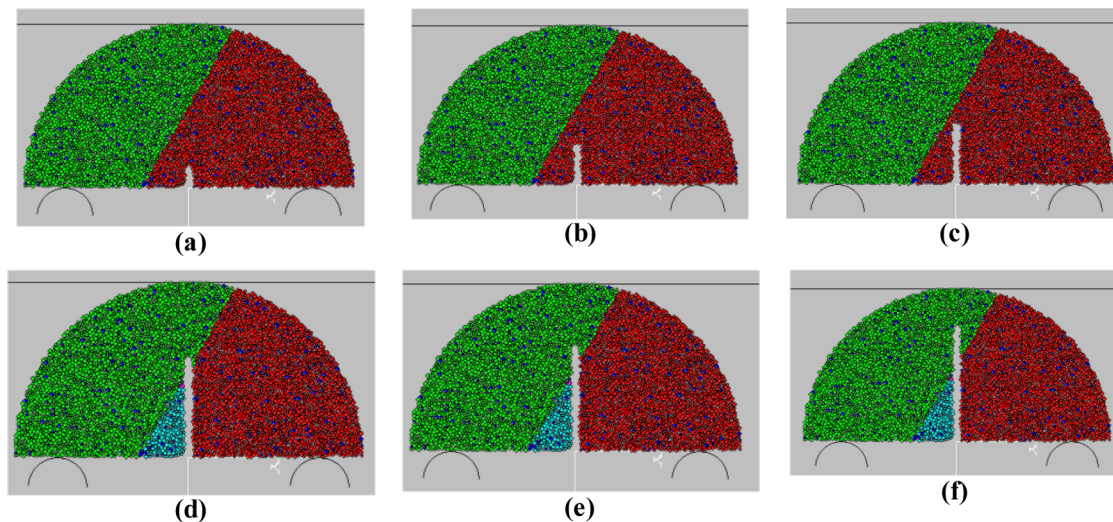


Fig. 9 Model with interface angle of 30° and different joint lengths

lines and shear cracks are represented by black lines. The tensile mode of failures is more dominant at the interfaces where the induced tensile cracks get a chance to propagate in the modelled samples.

3.2.4 The Modelled Mortar–Mortar Interfaces in the SCB Specimens with 60° Interface Angle

Figure 17a–f illustrates the process of failure and fracture patterns in the simulated mortar–mortar interfaces of the

SCB specimens with 60° interface angle. The length of joints was changed as 0.5 cm (Fig. 17a), 1 cm (Fig. 17b), 2 cm (Fig. 17c), 3 cm (Fig. 17d), 3.5 cm (Fig. 17e) and 4 cm (Fig. 17f). The black lines show the shear cracks, while the red lines denote the tensile cracks (induced in the modelled samples during their failure). During the failure of the modelled sample, the tensile cracks initiate in the model interface and propagate along that. Also, the tensile cracks primarily originate from the tip of the edge crack and extend in the direction of the applied load toward the specimens' boundaries.

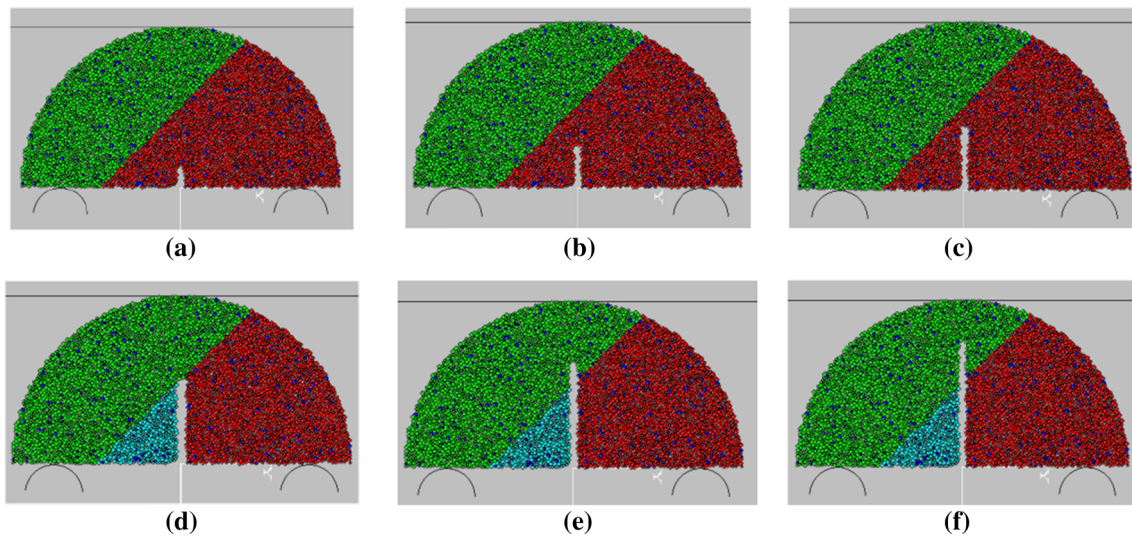


Fig. 10 Model with interface angle of 45° and different joint lengths

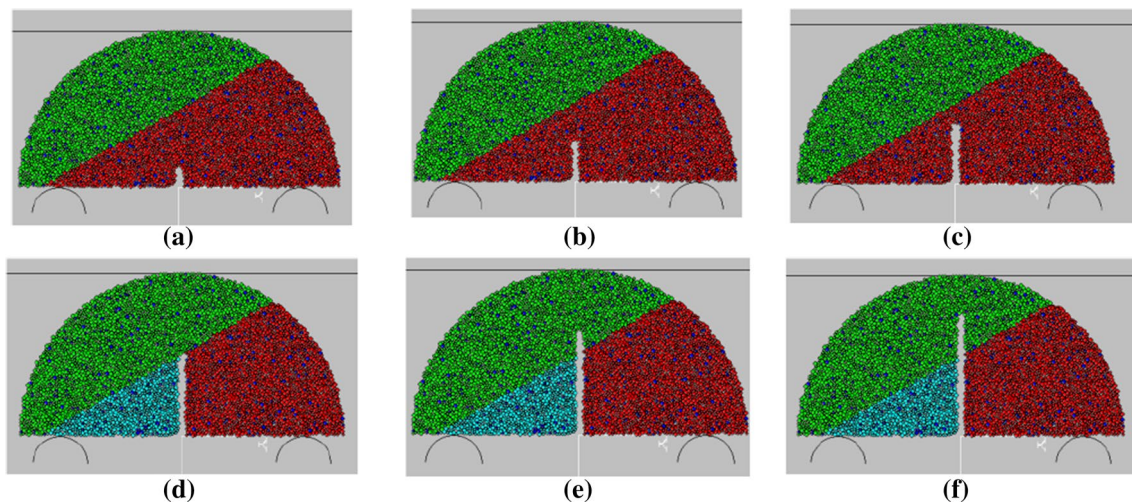


Fig. 11 Model with interface angle of 60° and different joint lengths

3.2.5 The Modelled Mortar–Mortar Interfaces in the SCB Specimens with 75° Interface Angle

Figure 18a–f demonstrates the failure, and fracture process in the simulated mortar–mortar SCB specimens with 75° interface angle. The length of joints (edge cracks) was 0.5 cm (Fig. 18a), 1 cm (Fig. 18b), 2 cm (Fig. 18c), 3 cm (Fig. 18d), 3.5 cm (Fig. 18e) and 4 cm (Fig. 18f). Here, the red lines denote the tensile and the black lines exhibit the shear cracks at the mortar–mortar interfaces. In these models, the tensile cracks induced in the mortar–mortar interface of the modelled SCB specimens and propagate along the interface during the specimen’s failure. These primary wing

(tensile) cracks may initiate from the tips of the cracks and extend parallel to the loading axis towards the specimens’ boundaries.

3.2.6 The Modelled Mortar–Mortar Interface Specimens with 90° Interface Angle

Figure 19a–f shows the fracture pattern of the mortar–mortar interface in the SCB modelled samples containing interface angles of 90° . The length of joints (edge cracks) was 0.5 cm (Fig. 19a), 1 cm (Fig. 19b), 2 cm (Fig. 19c), 3 cm (Fig. 19d), 3.5 cm (Fig. 19e) and 4 cm (Fig. 19f). In these models, the red lines denote the tensile cracks, while

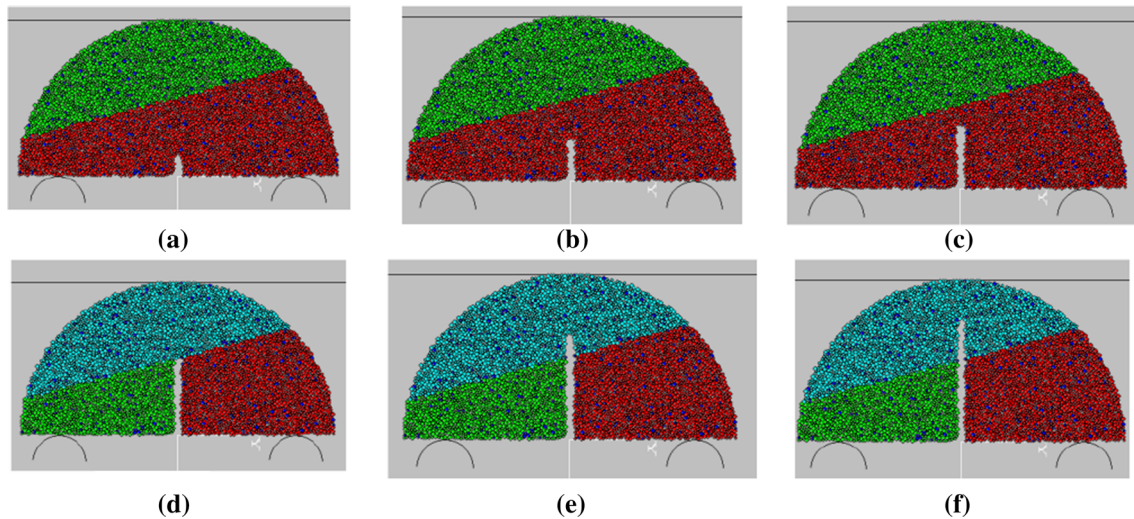


Fig. 12 Model with interface angle of 75° and different joint lengths

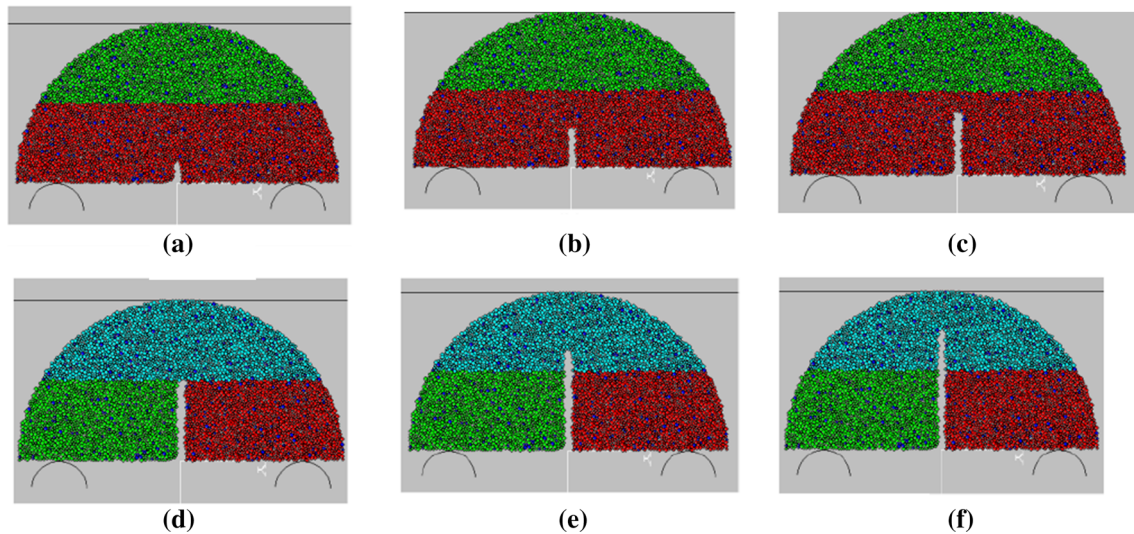


Fig. 13 Models for interface angle of 90° and different edge crack's lengths

shear cracks are elucidated by the black lines. These analyses show that the estimated failure mechanism of the modelled sample is mainly due to the initiated tensile cracks at the mortar–mortar interface which propagate along the interface of the modelled sample. Again, in this case, the primary wing cracks may start from the singular crack tips. They may further extend parallel to the loading axis and towards the model boundaries.

3.2.7 Modelling the Effects of Interface Angle and Length of Notch on the Failure of the SCB Specimens

Effects of the edge notch's (crack's) length and the mortar–mortar interface's angle on the maximum failure load

of the numerically modelled SCB specimens are graphically shown in Fig. 20. These numerical results explain that there is no change in the failure load for the interface angles of 15° , 30° and 45° as the joint length is increased but the failure load is decreased for the interface angles of 60° , 75° and 90° by increasing the joint (edge crack) length. On the other hand, the breaking loads of the SCB models were increased as the interface angles increased. It reaches a constant value for the interface angles of more than 60° .

Figure 21 shows the effects of joint's length and interface angle on the critical stress intensity factor, K_{IC} . Then, K_{IC} was numerically approximated for three different interface angles; 60° , 75° and 90° where the crack growth starts from

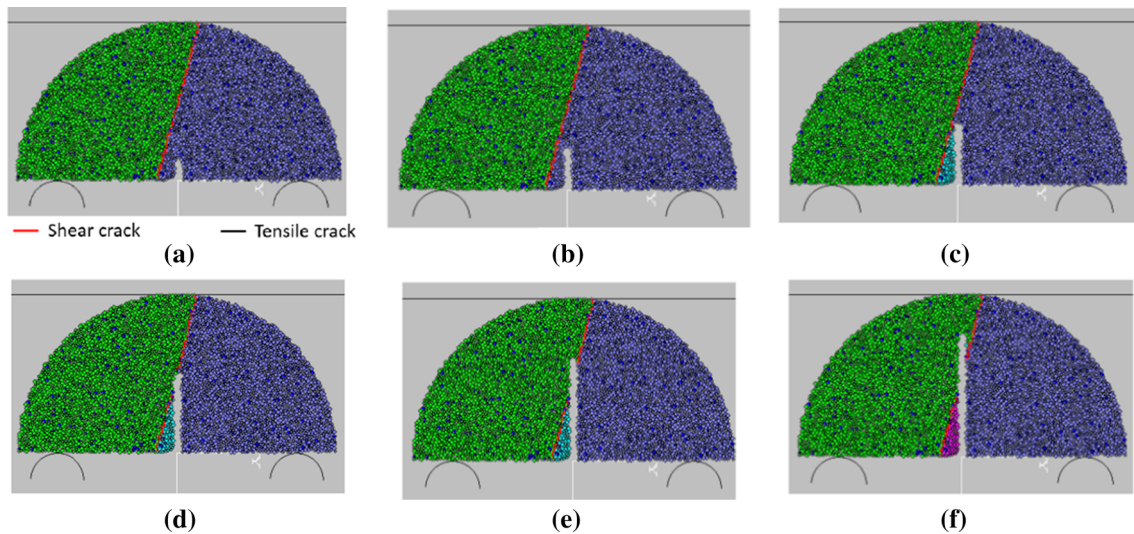


Fig. 14 Models considering interface angle of 15° and different joint lengths

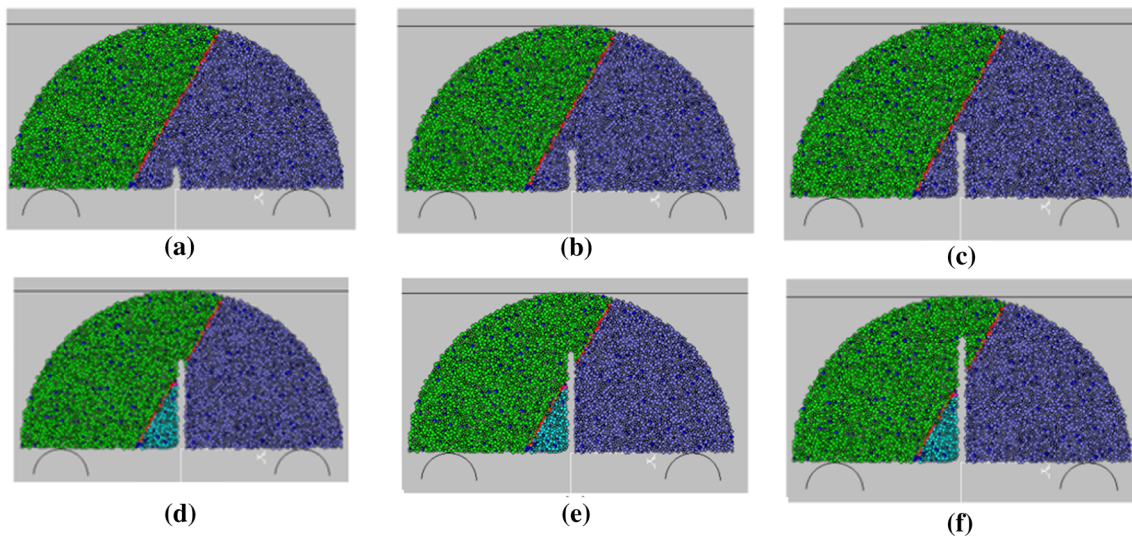


Fig. 15 Models considering interface angle of 30° and different joint lengths

the crack tip. However, these results show that the fracture toughness was constant by increasing the joint length.

4 Conclusions

The interaction between the edge crack and mortar–mortar interface in semi-circular bend specimens was studied. Various results were compared by performing the experimental

tests and the numerical simulations on the SCB specimens with different angles of mortar–mortar interface and different joint's lengths. The particle flow code for solving two-dimensional problems in geo-mechanics (PFC2D) was adopted to model the SCB specimens. The SCB Tests (with different angles of mortar–mortar interface and lengths of the edge cracks (joints)) were conducted in the laboratory. The accuracy of the approximated numerical results was validated by comparing them with their corresponding

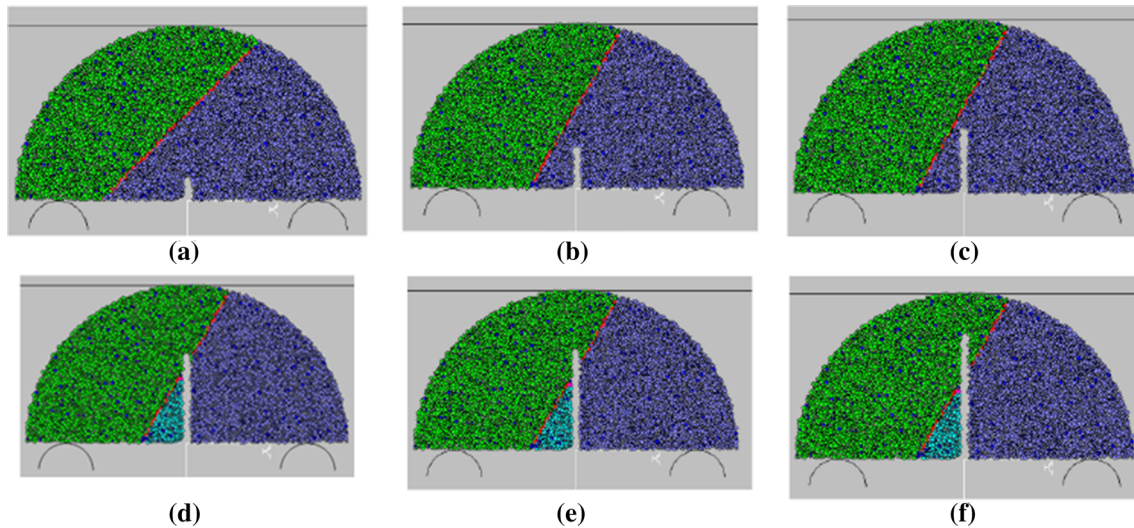


Fig. 16 Model with interface angle of 45° and different joint lengths

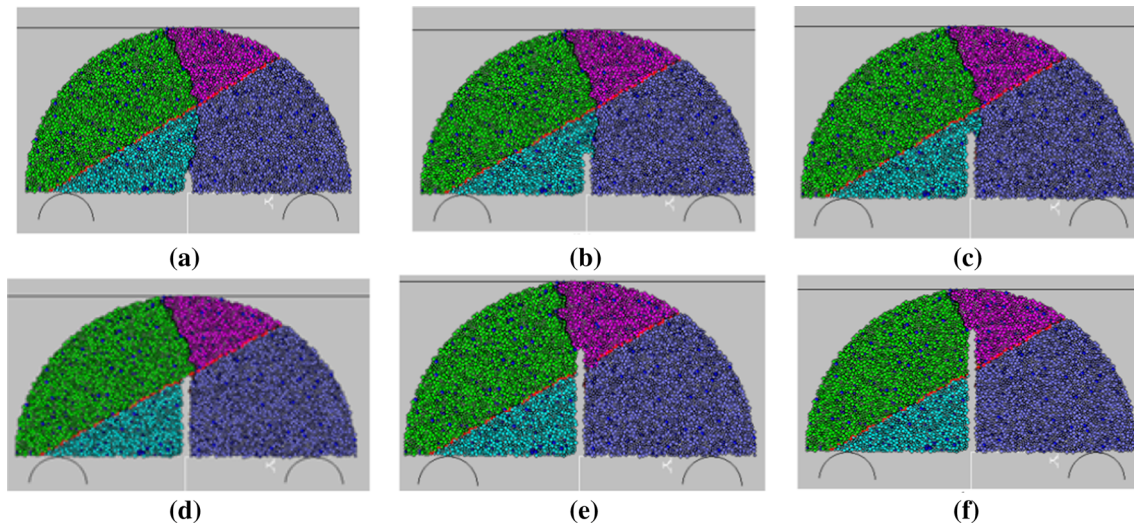


Fig. 17 Models with interface angle of 60° and different joint's (edge crack's) lengths

experimental values. However, the following conclusions may be gained from the results of these analyses:

- Three types of cracks are initiated in the SCB mortar samples i.e. tensile cracks, shear cracks and mixed tensile/shear cracks. When the angle of mortar–mortar interface is less than 30° , shear cracks are developed through the interface. When the angle of mortar–mortar interface is 45° , the mixed mode cracks are developed in both of
- the interface and intact material. When the angle of mortar–mortar interface is more than 45° , tensile cracks are dominantly developed in the intact material.
- The experimental and numerical failure patterns of SCB specimens with interface angles of 15° , 30° and 45° show that one wing crack starts from the edge crack tip and propagates through the model interface till reaches the model boundary.

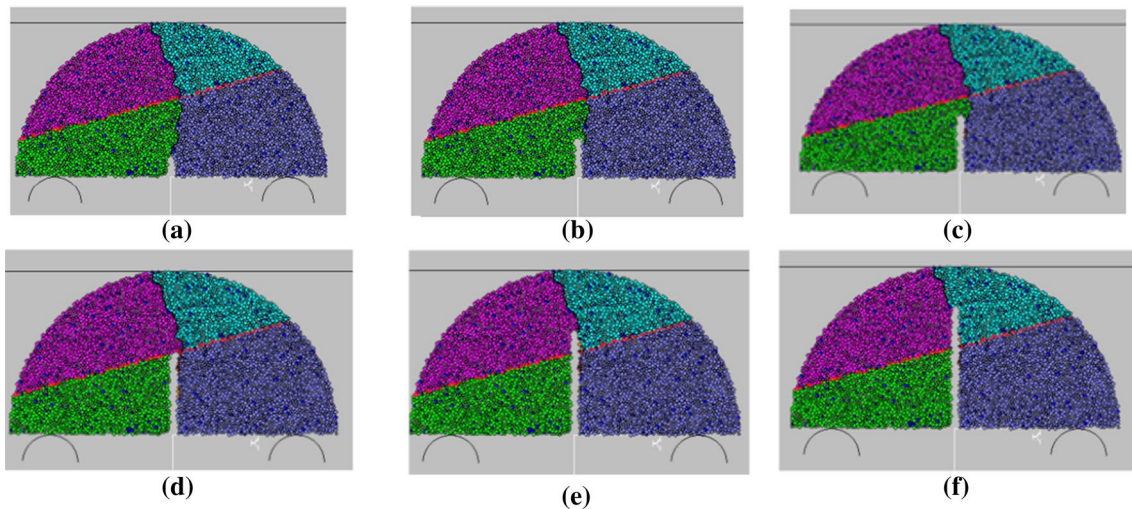


Fig. 18 Models with interface angle of 75° and different joint lengths

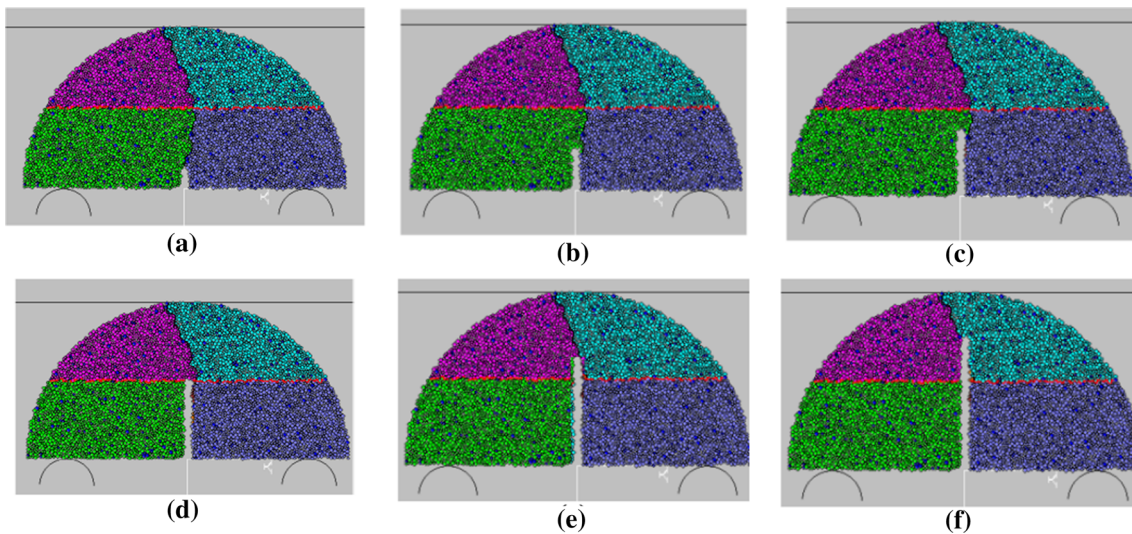


Fig. 19 Model with interface angle of 90° and different joint lengths

- The failure patterns of SCB specimens with interface angles of 60° , 75° and 90° , also demonstrate that wing cracks may initiate from the tip of the original cracks (joint) and propagate through the intact material till they meet the model boundary.
- Also, in most cases, a tensile wing crack may start its initiation from the crack tip and propagate towards the applied loading till touch the model boundary.
- When the interface angles are 15° , 30° and 45° (i.e. less than about 50°), the failure load approximately reaches a constant value as the joint's length increases.
- The failure load in the SCB test samples increased at the interface angles of 60° , 75° and 90° by increasing the joint's length
- As the inclination angle of the joint increased, the breaking load is also increased but it reaches a constant value when the inclination angles are above 60° .
- The fracture toughness is nearly constant as the joint's length is increased in the SCB samples.
- The corresponding failure processes are similar in both of the experimental tests and numerical simulations of the SCB mortar specimens.

Fig. 20 Effects of joint length and interface angle on the failure load of the modelled samples for six interface angles; 15°, 30°, 45°, 60°, 75° and 90°

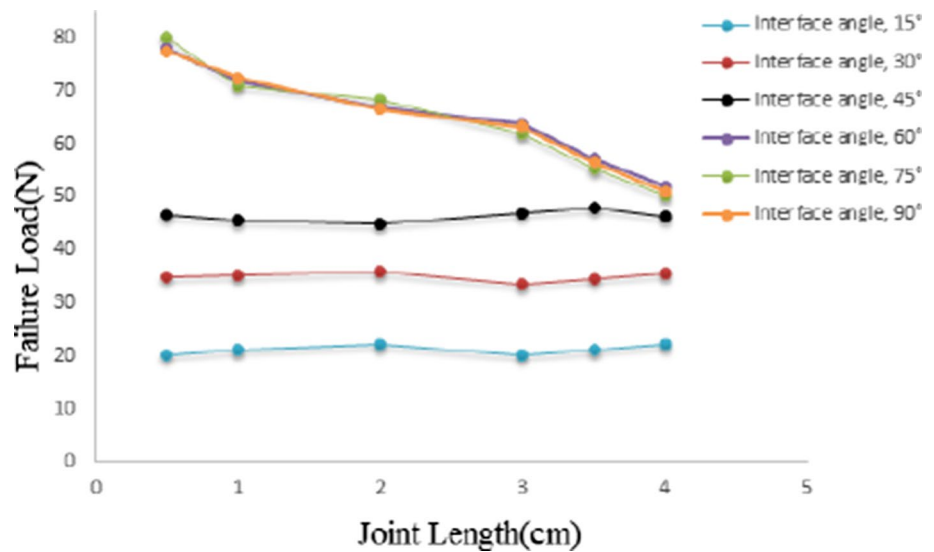
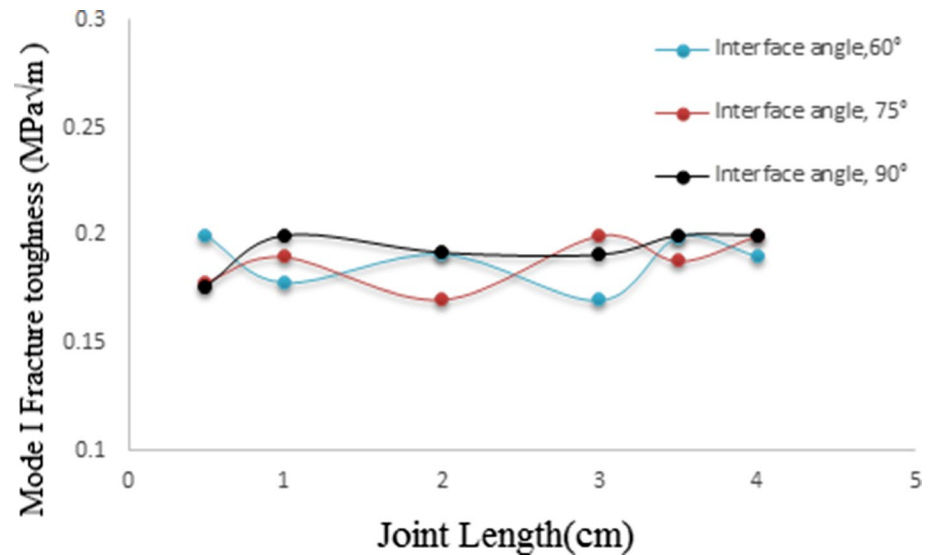


Fig. 21 Effects of the interface angle and crack length on the approximated fracture toughness of the simulated SCB tests for three interface angles; 60°, 75° and 90°



Acknowledgements This work was financially supported by National Natural Science Foundation of China (Grant No. 51608117), Key Specialized Research and Development Breakthrough Program in Henan province (Grant No. 192102210051).

References

- Adiyaman G, Yaylacı M, Birinci A (2015) Analytical and finite element solution of a receding contact problem. *Struct Eng Mech* 54(1):69–85
- Bi J, Zhou XP (2016) The 3D numerical simulation for the propagation process of multiple pre-existing flaws in rock-like materials subjected to biaxial compressive loads. *Rock Mech Rock Eng* 49:1611–162
- Chen F, Cao P, Rao QH, Ma CD, Sun ZQ (2005) A mode II fracture analysis of double edge cracked Brazilian disk using the weight function method. *Int J Rock Mech Min Sci* 42(3):461–465
- Chen CH, Chen CS, Wu JH (2008) Fracture toughness analysis on cracked ring disks of anisotropic rock. *Rock Mech Rock Eng* 41(4):539–562
- Cui ZD, Liu DA, An GM, Sun B, Zhou M, Cao FQ (2010) A comparison of two ISRM suggested chevron notched specimens for testing mode-I rock fracture toughness. *Int J Rock Mech Min Sci* 47:871–876
- Dai F, Chen R, Iqbal MJ, Xia K (2010) Dynamic cracked chevron notched Brazilian disk method for measuring rock fracture parameters. *Int J Rock Mech Min Sci* 47:606–613
- Dai F, Xia K, Zheng H, Wang Y (2011a) Determination of dynamic rock mode-I fracture parameters using cracked chevron notched semi-circular bend specimen. *Eng Fract Mech* 78(15):2633–2644
- Dastgerdi AS, Peterman RJ, Savic A, Riding K, Beck BT (2020) Prediction of splitting crack growth in prestressed concrete members using fracture toughness and concrete mix design. *Constr Build Mater* 246:118523. <https://doi.org/10.1016/j.conbuildmat.2020.118523>

- Du H, Dai F, Xia K, Xu N, Xu Y (2017) Numerical investigation on the dynamic progressive fracture mechanism of cracked chevron notched semi-circular bend specimens in split Hopkinson pressure bar tests. *Eng Fract Mech* 184:202–217
- Fang K, Fall M (2020) Insight into the mode I and mode II fracture toughness of the cemented backfill-rock interface: Effect of time, temperature and sulphate. *Constr Build Mater* 262:120860. <https://doi.org/10.1016/j.conbuildmat.2020.120860>
- Fowell RJ, Chen JF (1990) The third chevron-notch rock fracture specimen—the cracked chevron-notched Brazilian disk. In: *Proceedings 31st US symposium rock*. Balkema, Rotterdam, pp 295–302
- Fowell RJ, Xu C, Dowd PA (2006) An update on the fracture toughness testing methods related to the cracked chevronnotched Brazilian disk (CCNBD) specimen. *Pure Appl Geophys* 163:1047–1057
- Ghazvinian A, Nejati HR, Sarfarazi V, Hadei MR (2013) Mixed mode crack propagation in low brittle rock-like materials. *Arab J Geosci* 6:4435–4444
- Golewski GL (2019a) Estimation of the optimum content of fly ash in concrete composite based on the analysis of fracture toughness tests using various measuring systems. *Constr Build Mater* 213:142–155
- Golewski GL (2019b) The influence of microcrack width on the mechanical parameters in concrete with the addition of fly ash: consideration of technological and ecological benefits. *Constr Build Mater* 197:849–861
- Golewski GL (2021a) Validation of the favorable quantity of fly ash in concrete and analysis of crack propagation and its length – Using the crack tip tracking (CTT) method – In the fracture toughness examinations under Mode II, through digital image correlation. *Constr Build Mater* 296:122362. <https://doi.org/10.1016/j.conbuildmat.2021.122362>
- Golewski G (2021b) Studies of fracture toughness in concretes containing fly ash and silica fume in the first 28 days of curing. *Materials* 14(2):319–326
- Golewski G (2021c) Evaluation of fracture processes under shear with the use of DIC technique in fly ash concrete and accurate measurement of crack paths lengths with the use of a new crack tip tracking method. *Measurement* 181:109632
- Golewski GL, Sadowski T (2017) The fracture toughness the KIIIc of concretes with F fly ash (FA) additive. *Constr Build Mater* 143:444–454
- Haeri H, Sarfarazi V, Bagher Shemirani A, Hedayat A (2017) Experimental and numerical investigation of the center-cracked horse-shoe disk method for determining the mode I fracture toughness of rock-like material. *Rock Mech Rock Eng*. <https://doi.org/10.1007/s00603-017-1310-3>
- Hu J, Wen G, Lin Q, Cao P, Li S (2020) Mechanical properties and crack evolution of double-layer composite rock-like specimens with two parallel fissures under uniaxial compression. *Theoret Appl Fract Mech* 108:102610. <https://doi.org/10.1016/j.tafmec.2020.102610>
- Iqbal MJ, Mohanty B (2007) Experimental calibration of ISRM suggested fracture toughness measurement techniques in selected brittle rocks. *Rock Mech Rock Eng* 40(5):453–475
- Kataoka M, Obara Y, Kuruppu M (2014) Estimation of Fracture Toughness of anisotropic rocks by semi-circular bend (SCB) tests under water vapor pressure. *Rock Mech Rock Eng* 48:1353–1367
- Keles C, Tutluoglu L (2011) Investigation of proper specimen geometry for mode I fracture toughness testing with flattened Brazilian disc method. *Int J Fract* 169(1):61–75
- Kourkoulis SK, Markides CF, Chatzistergos PE (2012) The Brazilian disc under parabolically varying load: Theoretical and experimental study of the displacement field. *Int J Solids Struct* 49(7–8):959–972
- Kuruppu MD, Chong KP (1986) New specimens for modes I and II fracture investigations of geometries. In: *Proceedings of the Society of Experimental Mechanics*. Spring Conference on Experimental Mechanics, New Orleans, USA. pp 31–38
- Kuruppu MD, Chong KP (2012) Fracture toughness testing of brittle materials using semi-circular bend (SCB) specimen. *Eng Fract Mech* 91:133–150
- Kuruppu MD, Obara Y, Ayatollahi MR, Chong KP, Funatsu T (2014) ISRM-suggested method for determining the mode I static fracture toughness using semi-circular bend specimen. *Rock Mech Rock Eng* 47(1):267–274
- Li Y, Zhou H, Zhu W, Li S, Liu J (2015) Numerical study on crack propagation in brittle jointed rock mass influenced by fracture water pressure. *Mater* 8(6):3364–3376
- Lv LS, Wang JY, Xiao RC, Fang MS, Tan Y (2021) Influence of steel fiber corrosion on tensile properties and cracking mechanism of ultra-high performance concrete in an electrochemical corrosion environment. *Constr Build Mater* 278:122338. <https://doi.org/10.1016/j.conbuildmat.2021.122338>
- Markides CF, Kourkoulis SK (2020) Mathematical formulation of an analytic approach to the stress field in a flattened Brazilian disc. *Proc Struct Integr* 28:710–719
- Öner E, Yaylaci M, Birinci A (2015) Analytical solution of a contact problem and comparison with the results from FEM. *Struct Eng Mech* 54(4):607–622
- Saha I, Sagar RV (2021) Classification of the acoustic emissions generated during the tensile fracture process in steel fibre reinforced concrete using a waveform-based clustering method. *Constr Build Mater* 294:123541. <https://doi.org/10.1016/j.conbuildmat.2021.123541>
- Sarfarazi V, Faridi HR, Haeri H, Schubert W (2016) A new approach for measurement of anisotropic tensile strength of concrete. *Adv Concrete Constr* 3(4):269–284
- Shemirani B, Naghdabadi A, Ashrafi R (2016) Experimental and numerical study on choosing proper pulse shapers for testing concrete specimens by split Hopkinson pressure bar apparatus. *Constr Build Mater* 125:326–336
- Shen Q-Q, Rao Q-H, Li Z, Yi W, Sun D-L (2021) Interacting mechanism and initiation prediction of multiple cracks. *Trans Nonferrous Metals Soc China* 31(3):779–791
- Shiryayev AM, Kotkis AM (1982) Methods for determining fracture toughness of brittle porous materials. *Ind Lab* 48(9):917–918
- Shou Y, Zhou XP (2019a) A coupled thermomechanical nonordinary state-based peridynamics for thermally induced cracking of rocks. *Fatigue Fract Eng Mater Struct* 23:89–97
- Shou Y, Zhou XP (2019b) 3D numerical simulation of initiation, propagation and coalescence of cracks using the extended non-ordinary state-based peridynamics. *Theoret Appl Fract Mech* 101:254–268
- Shou Y, Zhou XP (2021) A coupled hydro-mechanical non-ordinary state-based peridynamics for the fissured porous rocks. *Eng Anal Boundary Elem* 123:133–146
- Tang T, Bažant ZP, Yang S, Zollinger D (1996) Variable-notch onesize test method for fracture energy and process zone length. *Eng Fract Mech* 55(3):383–404
- Tutluoglu L, Keles C (2011) Mode I fracture toughness determination with straight notched disk bending method. *Int J Rock Mech Min Sci* 48(8):1248–1261
- Vălean C, Marşavina L, Mărghiţaş M, Linul E, Razavi J, Berto F, Brighenti R (2020) The effect of crack insertion for FDM printed PLA materials on Mode I and Mode II fracture toughness. *Proc Struct Integr* 28:1134–1139
- Wang QZ, Gou XP, Fan H (2012) The minimum dimensionless stress intensity factor and its upper bound for CCNBD fracture toughness specimen analyzed with straight through crack assumption. *Eng Fract Mech* 82:1–8

- Wang Z, Li Y, Cai W, Zhu W, Kong W, Dai F, Wang C, Wang K (2021) Crack propagation process and acoustic emission characteristics of rock-like specimens with double parallel flaws under uniaxial compression. *Theoret Appl Fract Mech* 114:102983. <https://doi.org/10.1016/j.tafmec.2021.102983>
- Wei MD, Dai F, Xu NW, Xu Y, Xia K (2015) Three-dimensional numerical evaluation of the progressive fracture mechanism of cracked chevron notched semi-circular bend rock specimens. *Eng Fract Mech* 134:286–303
- Yang SQ (2015) An experimental study on fracture coalescence characteristics of brittle sandstone specimens combined various flaws. *Geomech Eng* 8(4):541–557. <https://doi.org/10.12989/gae.2015.8.4.541>
- Yaylac M (2016) The investigation crack problem through numerical analysis. *Struct Eng Mech* 57(6):1143–1156
- Yaylac M (2016) The investigation crack problem through numerical analysis. *Struct Eng Mech* 57(6):1143–1156
- Yaylac M, Birinci A (2013) The receding contact problem of two elastic layers supported by two elastic quarter planes. *Struct Eng Mech* 48(2):241–255
- Yaylac M, Avcar M (2020) Finite element modeling of contact between an elastic layer and two elastic quarter planes. *Comput Concr* 26(2):107–111
- Yaylac M, Eyüboğlu A, Adıyaman G, Yaylacı EU, Öner E, Birinci A (2021a) Assessment of different solution methods for receding contact problems in functionally graded layered mediums. *Mech Mater* 32(3):66–78. <https://doi.org/10.1016/j.mechmat.2020.103730>
- Yaylacı M, Yaylı M, Yaylacı EU, Ölmez H, Birinci A (2021b) Analyzing the contact problem of a functionally graded layer resting on an elastic half plane with theory of elasticity, finite element method and multilayer perceptron. *Struct Eng Mech* 78(5):585–597
- Yaylacı M, Adıyaman E, Öner E, Birinci A (2021c) Investigation of continuous and discontinuous contact cases in the contact mechanics of graded materials using analytical method and FEM. *Comput Concr* 27(3):199–210
- Yu A, Andersen DH, He J, Zhang Z (2021) Is it possible to measure the tensile strength and fracture toughness simultaneously using flattened Brazilian disk? *Eng Fract Mech* 247:107633. <https://doi.org/10.1016/j.engfracmech.2021.107633>
- Zhang S, Li Y, Liu H, Ma X (2021) Experimental investigation of crack propagation behavior and failure characteristics of cement in filled rock. *Constr Build Mater* 268:121735. <https://doi.org/10.1016/j.conbuildmat.2020.121735>
- Zhou XP (2014) An experimental study of crack coalescence behaviour in rock-like materials containing multiple flaws under uniaxial compression. *Rock Mech Rock Eng* 47:1961–1986
- Zhou YX, Xia K, Li XB, Li HB, Ma GW, Zhao J, Zhou ZL, Dai F (2012) Suggested methods for determining the dynamic strength parameters and mode-I fracture toughness of rock materials. *Int J Rock Mech Min Sci* 49:105–112
- Zhou XP, Bi J, Qian QH (2015) Numerical simulation of crack growth and coalescence in rock-like materials containing multiple pre-existing flaws. *Rock Mech Rock Eng* 48(3):1097–1114